NUMERICAL SIMULATION OF SUPERSONIC COMBUSTION WITH CH_4-H_2 FUEL

D.M. Davidenko, I. Gökalp
Centre National de la Recherche Scientifique – Laboratoire de Combustion et Systèmes Réactifs (CNRS-LCSR), Orléans, France

E. Dufour
MBDA-France, Châtillon, France

P. Magre
Office National d'Études et de Recherches Aérospatiales (ONERA), Palaiseau, France

Supersonic combustion of methane-hydrogen (CH_4-H_2) fuel in a combustion chamber model has been studied numerically. For this purpose, a reduced kinetic mechanism was elaborated and integrated into a Navier-Stokes code. The simulation conditions corresponded to a supersonic combustion chamber, which was previously tested on the experimental facility LAERTE at ONERA. Computational results on the supersonic combustion have been obtained for various mass fractions of H_2 in fuel ranging from 20 % to 100 %.

Introduction

MBDA-France and ONERA conduct a joint project aimed at flight tests of a hypersonic demonstrator at flight Mach numbers from 4 to 8 [1]. The demonstrator will be powered by a scramjet engine dedicated to the study of the drag-to-thrust balance and validation of the design and ground test methodologies.

Among possible fuels, CH_4-H_2 mixture is considered for the demonstrator because its chemistry is well known and its ignition and combustion properties can be widely varied by changing the component fractions.

Computational fluid dynamics (CFD) is considered as one of the main means for the scramjet performance prediction. Since CFD codes incorporate diverse models, they must be validated for representative test cases provided by basic studies. Some of basic supersonic combustion tests were realized at ONERA on the experimental facility LAERTE. The experimental tests were performed with different fuels such as H_2, C_2H_4, and CH_4-H_2 mixture. Experimental data on the H_2 combustion [2, 3, 4] were used in several studies for the comparison with numerical simulation results [5, 6].

CNRS-LCSR takes part in the development of computational models to be integrated into CFD codes used by MBDA-France and ONERA. CNRS-LCSR obtained a Navier-Stokes code called MSD for this purpose. Some corrections have been introduced into the turbulence model to improve its perform-

ance when simulating round compressible jets [7]. A reduced chemistry kinetic model was developed and incorporated into the code MSD for the CH_4-H_2 combustion [8]. Since the first publication, the CH_4-H_2 chemistry model has been revised and refined [9]. Its application to the supersonic combustion simulation is the subject of the present work.

Supersonic combustion experiment

The supersonic combustion experiment was carried out at ONERA on the test facility LAERTE. The LAERTE configuration is shown schematically in fig. 1. The combustion chamber model was connected directly to a supersonic wind tunnel consisted of a flame heater and a supersonic nozzle.

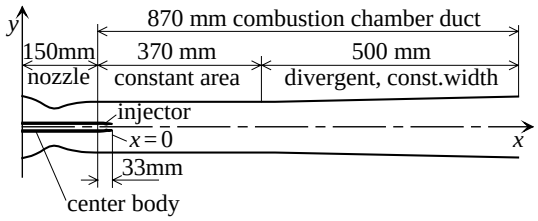

Fig. 1 LAERTE configuration.

The heater provided a hot flow of vitiated air with the following parameters: mass flow rate of 0.65 kg/s; total temperature of 1850 K; oxygen mole fraction of 21 %. The air flow was preheated up to 850 K in a resistance heater before coming to the flame heater, where it was enriched with oxygen and finally heated by burning some hydrogen.

The nozzle created a supersonic flow with the following design parameters: Mach number of 2, static pressure of 0.8 bar. The nozzle had two symmetric profiled walls and two flat sidewalls, all cooled with water.

A water-cooled axisymmetric fuel injector was installed along the combustion chamber axis passing through the nozzle duct. The injector had a 6 mm exit diameter and was designed to accelerate the fuel flow up to Mach 2.

The combustion chamber duct, made of refractory steel, was uncooled. It consisted of a constant area portion with a square cross section 45 mm × 45 mm and a divergent portion with a constant width of 45 mm and a half angle of 1.15° in the vertical plane (see fig. 1).

More details on the experimental facility can be found in [2-4, 6].

Numerical models

Numerical simulations of the supersonic combustion were realized by means of the code MSD. It was developed by ONERA for scientific and industrial applications in aerospace propulsion. The code was previously utilized to simulate LAERTE experiments with H_2 [6] and to make predictions on the CH_4-H_2 supersonic combustion [8].

This paper presents simulations performed with improved computational models and taking account for methodological considerations discussed in [6]. The used numerical schemes and models were described in general in [6]. Only specific features of the computational models are addressed here.

The k-ε turbulence model had the standard parameter set but it was enhanced with the Sarkar compressibility correction and a modified version of the Pope correction (for reference see [7]). The turbulence model with the corrections was tested by simulating several compressible inert and reacting jets [7]. Based on the test results, the turbulent Prandtl and Schmidt numbers were taken equal to 0.8.

The chemistry model was represented by the reduced kinetic mechanism including 21 reactive species: CH_4, H_2, O_2, CO_2, H_2O, H, O, OH, HO_2, H_2O_2, CO, HCO, CH_2O, CH_2, CH_3, CH_3O, C_2H_6, C_2H_5, C_2H_4, C_2H_3, C_2H_2.

The reduced mechanism was obtained from a skeletal mechanism with 123 reactions. A similar skeletal mechanism was considered in [8] but since that publication, several im-

provements have been made such as: updating of reaction rate parameters according to a newer version of LCSR natural gas mechanism by Dagaut [10]; introduction of pressure-dependent reaction rates; revision of 3rd body efficiencies.

The skeletal mechanism was further reduced via the reaction sensitivity analysis. The authors developed and applied an automatic procedure for reaction elimination [9] that identified 80 important reactions. The reactions were tested by simulating the autoignition in a homogeneous constant-pressure reactor. The domain of test conditions was defined as follows: pressure 0.1-10 bar; initial temperature 1000-2000 K; fuel equivalence ratio 0.25-4; H_2 mass fraction in fuel 0-0.5.

To make the reduced chemistry model more efficient in CFD applications, the quasi-steady state (QSS) approximation was applied to some reactive species. The net production rate of a QSS species is supposed to be 0 so its concentration can be determined from an algebraic equation, instead of solving a differential one. The QSS assumption is valid if the contribution of chemical factors to the species mass balance is much greater than that of convection and diffusion processes, and associated chemical time scales are much shorter compared to the other species.

Examination of concentration profiles and the role of species in the mechanism indicated that 5 species namely H_2O_2, CH_2, CH_3O, C_2H_5, and C_2H_3 could be assumed in the QSS. These species have no common reactions thus their concentrations can be expressed explicitly though the concentrations of non-QSS species. Computational tests confirmed that the QSS approximation is correct for all the 5 species.

No coupling was assumed between the turbulence and chemical kinetics thus the reaction rates were calculated for mean temperature and species concentrations.

Computational cases

Simulations of the CH_4-H_2 combustion could be conducted only in a 2D approximation because of limited computational resources. Thus for the combustion chamber geometry, we adopted a simplified approach, which consisted in the substitution of a 2D axisymmetric configuration for the real 3D shape. The duct profile was adjusted to have cross-section areas equivalent to the real geometry. The injector configuration being axisymmetric remained unchanged. A previous analysis of 2D and 3D simulations of the H_2 combustion demonstrated a very satisfactory general agreement with some local differences [9].

Solutions were obtained on a fine computational mesh with a minimum cell size of 0.05 mm in both spatial directions. The main computational domain, downstream from the injection station, had 750 cells in the longitudinal direction and 200 cells in the transversal one, 1.5×10^5 cells in total.

Initial parameter profiles were obtained from computations of the nozzle and injector channels. Temperature distributions were imposed on the wall boundaries. The wall temperature rose from 500 K to 1000 K along the constant area duct and further decreased to 900 K in the divergent duct. A constant temperature of 1000 K was imposed on the external wall of the center body.

Simulations were made for 5 fuel compositions. Table 1 presents fuel feed parameters such as the mass flow rate, G_{fuel}, overall equivalence ratio, ϕ_{fuel}, and calorific power, Q_{fuel}, depending on the mass fraction of H_2 in fuel, η.

For $\eta = 1$ and 0.51, the experimental mass flow rate was taken. For the other compositions, G_{fuel} was evaluated providing a static pressure of 0.8 bar at the injector exit. The calorific power was estimated from the standard calorific capacities of H_2 and CH_4.

Table 1

η	G_{fuel}, g/s	ϕ_{fuel}	Q_{fuel}, kW
1	6.2	0.307	744
0.51	8.1	0.304	694
0.4	9.5	0.330	741
0.3	10.5	0.340	747
0.2	12.0	0.357	766

The computations were conducted on a PC cluster operating under the Linux system with the parallel environment MPICH. One computational job was shared between 8 processors working at 3 GHz. One simulation needed 8000 iterations that corresponded to a real time about 43 hours.

Results and discussion

Combustion of pure H_2

The computational approach is validated by comparing experimental and simulation results in case of the H_2 combustion. Wall pressure distributions are shown in fig. 2. Pressure values are normalized by the total pressure in the heater.

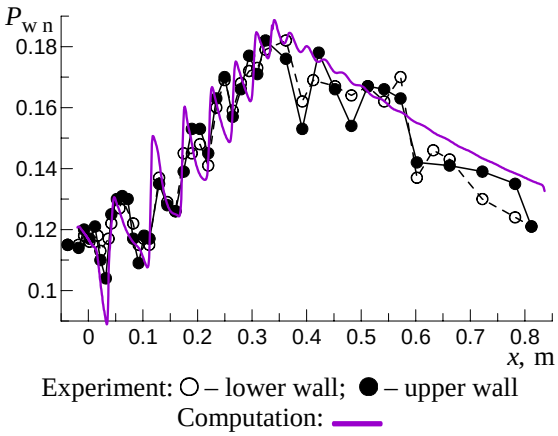

Fig. 2 Wall pressure distributions at H_2 combustion.

The agreement between the experiment and simulation is good indicating that the overall heat release is predicted correctly. Pressure fluctuations are well reproduced in the constant area duct ($x < 0.34$ m) where the pressure rises. In the divergent duct ($x > 0.34$ m), experimental pressure distributions feature considerably more intense fluctuations than the computed ones. This fact may be explained by a certain displacement of the injector from the axial position and by duct wall deformations cased by thermal stresses.

Combustion of CH_4-H_2 fuel with $\eta = 0.51$

Computational results on the Mach number, M, total temperature, T_t, and species mass fractions, Y_{CH4}, Y_{H2}, Y_{CO}, Y_{CO2}, Y_{H2O}, are presented in fig. 3 for the CH_4-H_2 combustion with $\eta = 0.51$. Parameter fields, being symmetric, are shown only above the axis.

Within each parameter field, a white line traces the stoichiometric surface, which remains far from the axis. At $x = 0.8$ m, the equivalence ratio on the axis is about 4.8. These two facts indicate rather a poor overall mixing.

The Mach number field shows that the flow is supersonic except for some transonic spots localized within the fuel-rich zone. One can note also the presence of expansion waves followed by recompression shocks, which are generated by the center-body profile and interaction between the main stream and fuel jet. The expansion and shock waves travel downstream producing pressure fluctuations similar to those shown in fig. 2.

The total temperature field features several distinct regions: cold jet core and mixing zone around the axis (blue colors); cooled boundary layers near the walls of the center body and chamber duct (green colors); hot combustion zone (yellow and red colors). The self-ignition takes place at $x \approx 0.15$ m in the fuel-lean zone. The temperature maximum then installs near the stoichiometric surface. Expanding combustion products narrow the passage for the fuel jet and air flow and cause a noticeable decrease of the overall Mach number in the constant area duct.

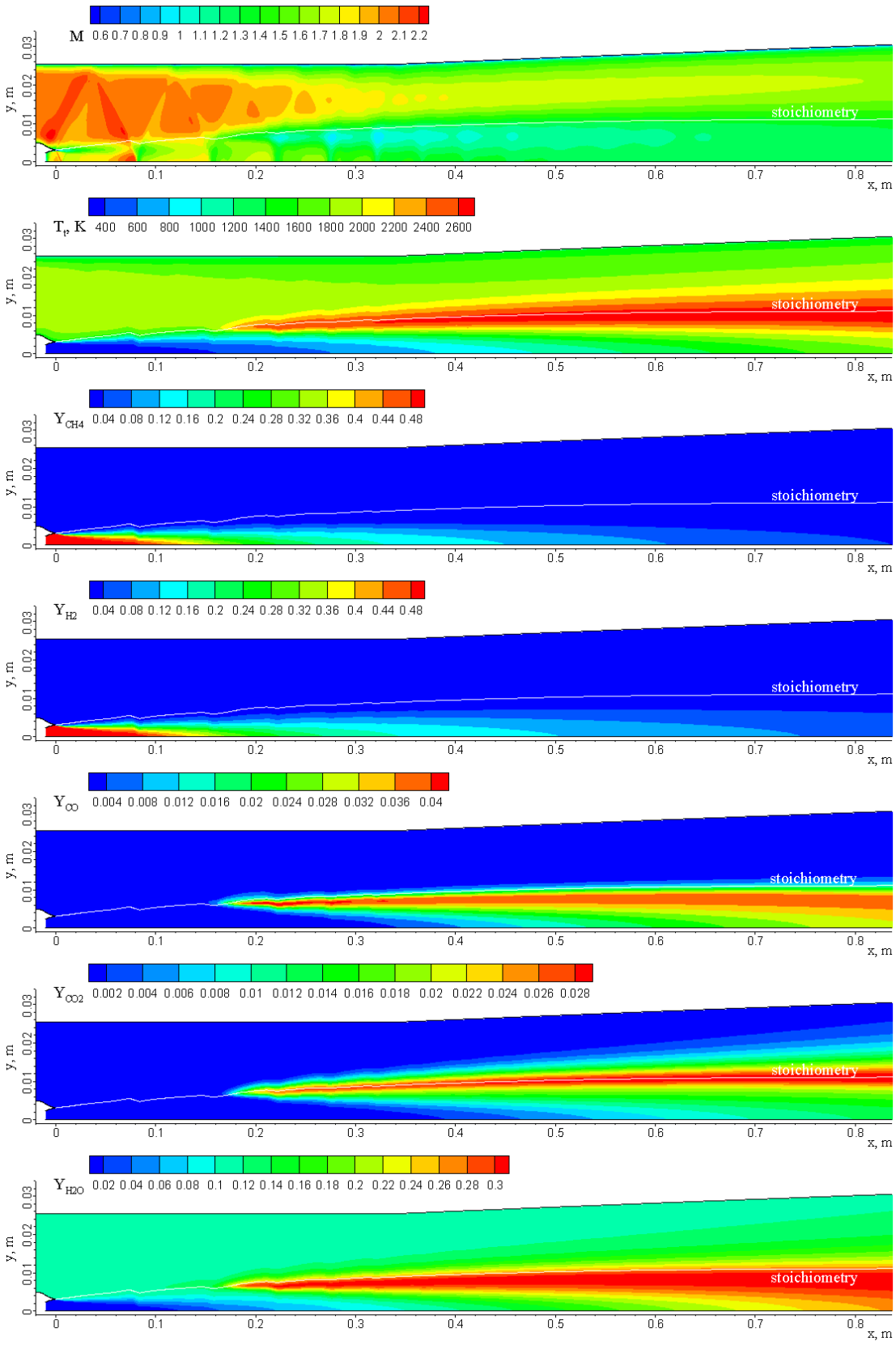

Fig. 3 Computed parameter fields corresponding to the CH_4-H_2 combustion with $\eta = 0.51$.

The mass fractions of CH_4 and H_2 have similar fields. However Y_{CH4} decreases more rapidly in the fuel-rich zone because of faster thermal decomposition and partial oxidation of CH_4. It is not seen in fig. 3 but it was previously found that H_2 is consumed preferentially in the fuel-lean zone before the ignition [11].

CO, one of the most abundant intermediate species, mainly forms in the fuel-rich zone. Then CO is consumed by reactions producing CO_2 whose maximum concentration is near the stoichiometric surface. The maximum of H_2O is in the fuel-rich zone where O_2 is fully depleted. Formation of CO_2 and H_2O provides major exothermic effect so that the hot zone in the total temperature field corresponds to the superposition of the zones with high concentrations of these species.

From a close examination of the Y_{H2O} field, one can find out the beginning of H_2O production at $x \approx 0.1$ m, i.e. somewhat earlier than the quick rise of the total temperature. This fact indicates that in the fuel-lean zone, where H_2 is preferentially consumed, the H_2 oxidation causes some thermal effect.

From the experimental measurements of the wall pressure, we estimated the ignition distance and found it close to the simulation result. The experimental data on the CH_4-H_2 combustion are not available for the publication so we do not illustrate them.

Effect of the fuel composition

Computed distributions of the wall pressure are presented in fig. 4 for the five fuel compositions given in Table 1.

The same simulations are represented in fig. 5 by distributions of the maximum total temperature $T_{t\,max}$ and mass-average total temperature $T_{t\,avr}$, which illustrate the combustion process development.

When the CH_4 fraction in fuel increases, the ignition delay first grows by 50% ($\eta = 0.51$), then it doubles ($\eta = 0.4$) and triples ($\eta = 0.3$). At $\eta = 0.2$, there is no ignition at all. This last observation contradicts the results of the previous simulations [8, 11] that showed the presence of combustion at $\eta = 0.2$. This disagreement is because of different boundary conditions and computational meshes. In the previous simulations, the walls were supposed adiabatic including the center-body wall, in addition the mesh was significantly coarser. Both factors can effectively accelerate the simulated ignition process. Problems associated with the boundary conditions were addressed in [6].

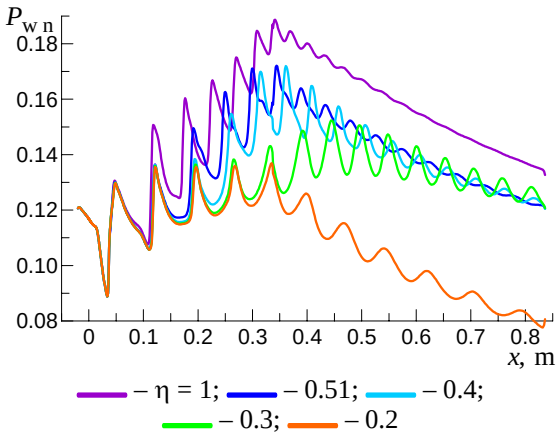

Fig. 4 Wall pressure distributions at various η.

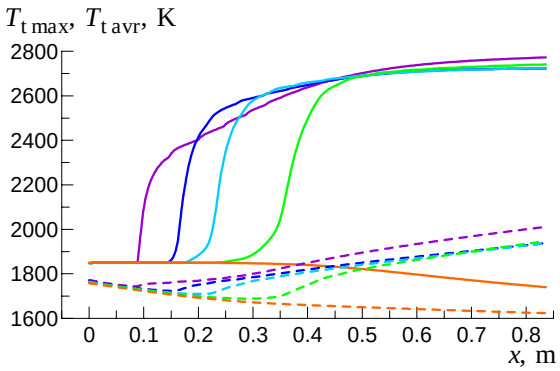

Solid lines – $T_{t\,max}$; dashed lines – $T_{t\,avr}$.

Fig. 5 Distributions of maximum and average total temperatures at various η.

The curves of $T_{t\,max}$ indicate that the combustion starts later at smaller η, nevertheless $T_{t\,max}$ gets to the same final level.

The wall pressure distributions follow the

overall heat release illustrated by the evolution of $T_{t\,avr}$. At $\eta = 1$, the wall pressure at the duct end is higher than at $\eta = 0.51$ by several reasons: greater Q_{fuel}; more complete mixing; faster formation of combustion products due to the rapid chemistry. When η decreases from 0.51 to 0.2, the available calorific power grows, but the final pressure level is practically constant being in agreement with the average total temperature. A detailed analysis shows, that the efficiency of fuel mixing and fuel chemical consumption are practically the same. However the process of combustion product formation becomes less intense (effects of slower chemistry and duct expansion) and the residence time after the ignition decreases as well. As a result, the growth of the available calorific capacity is compensated by the reduction of the combustion efficiency.

Acknowledgments

This study was carried out thanks to the financial support of MBDA-France and the Research Federation EPEE. The computational resources were provided by the Federation EPEE.

References

[1] Serre L, Falempin F. LEA flight test program: a first step to an operational application of high-speed airbreathing propulsion, *12th AIAA Int. Space Planes and Hypersonic Systems and Technologies Conf.*, AIAA-2003-7031, Norfolk, VA, Dec. 15-19, 2003.

[2] Magre P, Bouchardy P. Nitrogen and hydrogen coherent anti-Stokes Raman scattering thermometry in a supersonic reactive mixing layer, *Proc. of the Combustion Institute*, Vol. 28, pp 697-703, 2000.

[3] Bresson A, Bouchardy P, Magre P, Grisch F. OH/acetone PLIF and CARS thermometry in a supersonic reactive layer, *10th AIAA/NAL/NASDA/ISAS Int. Space Planes and Hypersonic Systems and Technologies Conf.*, AIAA-2001-1759, Kyoto, Japan, Apr. 24-27, 2001.

[4] Weisgerber H, Martinuzzi R, Brummund U, Magre P. Mesures de vitesse par PIV dans une combustion supersonique hydrogène-air à Mach 2, *37e Colloque d'Aérodynamique Appliquée "Aérodynamique et Propulsion des véhicules à grande vitesse,"* Arcachon, France, Mar. 28-30, 2001.

[5] Gaffié D, Wepler U, Magre P, Koschel W, Novelli P. Numerical instigation of supersonic reacting hydrogen jets in a hot air coflow, *10th AIAA/NAL/NASDA/ISAS Int. Space Planes and Hypersonic Systems and Technologies Conf.*, AIAA-2001-1864, Kyoto, Japan, Apr. 24-27, 2001.

[6] Davidenko D M, Gökalp I, Dufour E, Magre P. Numerical simulation of hydrogen supersonic combustion and validation of computational approach, *12th AIAA Int. Space Planes and Hypersonic Systems and Technologies Conf.*, AIAA-2003-7033, Norfolk, VA, Dec. 15-19, 2003.

[7] Davidenko D M, Gökalp I, Dufour E, Magre P. Numerical modeling of inert and reacting compressible turbulent jets, *13th AIAA/CIRA Int. Space Planes and Hypersonic Systems and Technologies Conf.*, AIAA-2005-3237, Capua, Italy, May 16-20, 2005.

[8] Davidenko D M, Gökalp I, Dufour E, Gaffié D, Kinetic mechanism validation and numerical simulation of supersonic combustion of methane-hydrogen fuel, *11th AIAA/AAAF Int. Space Planes and Hypersonic Systems and Technologies Conf.*, AIAA-2002-5207, Orléans, France, Sep. 29 – Oct. 4, 2002.

[9] Davidenko D M, Gökalp I, Dufour E, Magre P. Ignition and Combustion of Hydrogen and Methane in a Model Supersonic Combustion Chamber, *Proceedings of the European Combustion Meeting*, ECM2005, Louvain-la-Neuve, Belgium, Apr. 3-6, 2005.

[10] Dagaut P. On the kinetics of hydrocarbons oxidation from natural gas to kerosene and diesel fuel, *Phys. Chem. Chem. Phys.*, Vol. 4, pp 2079-2094, 2002.

[11] Davidenko D M, Gökalp I, Dufour E, Gaffié D, Numerical simulations of supersonic combustion of methane-hydrogen fuel in an experimental combustion chamber, *Parallel Computational Fluid Dynamics – Advanced Numerical Methods, Software and Applications*, pp 529-536, Elsevier B.V., 2004.